Oxytocin selectively excites interneurons and inhibits output neurons of the bed nucleus of the stria terminalis (BNST)

Running title: Oxytocin regulates intrinsic inhibitory network of the BNST

Walter Francesconi [1,2], Fulvia Berton [1,2], Valentina Olivera-Pasilio [1,2,3], and Joanna Dabrowska [1,2,3]

[1] Center for the Neurobiology of Stress Resilience and Psychiatric Disorders, Rosalind Franklin University of Medicine and Science, North Chicago, IL 60064, USA

[2] Discipline of Cellular and Molecular Pharmacology, Chicago Medical School, Rosalind Franklin University of Medicine and Science, North Chicago, IL 60064, USA

[3] School of Graduate and Postdoctoral Studies, Rosalind Franklin University of Medicine and Science, North Chicago, IL 60064, USA

* To whom correspondence should be addressed:

Joanna Dabrowska, Center for the Neurobiology of Stress Resilience and Psychiatric Disorders, Discipline of Cellular and Molecular Pharmacology, Chicago Medical School, Rosalind Franklin University of Medicine and Science, North Chicago, IL 60064, USA

joanna.dabrowska@rosalindfranklin.edu

Phone: (847) 578-8664

Fax: (847) 578-3268

Number of figures (5), Supplementary Information with supplementary Table

Abstract

The dorsolateral bed nucleus of the stria terminalis ($BNST_{DL}$) has high expression of oxytocin (OT) receptors (OTR), which were shown to facilitate cued fear. The $BNST_{DL}$ contains GABA-ergic neurons classified based on intrinsic membrane properties into three major types. Using *in vitro* patch-clamp recordings in male rats, we demonstrate that OT selectively excites Type I neurons in an OTR-dependent manner as revealed by a significantly increased resting membrane potential, increased input resistance, reduced rheobase, reduced fast and medium spike afterhyperpolarization, reduced threshold and latency to a first spike, as well as a left shift in the spike frequency/current relationship. As Type I neurons are putative $BNST_{DL}$ interneurons, we next recorded inhibitory synaptic transmission in all three types of neurons and we demonstrate that OT increases the frequency, but not amplitude, of spontaneous inhibitory post-synaptic currents (sIPSCs), selectively in Type II neurons. This effect was abolished by the presence of an OTR antagonist or tetrodotoxin, the latter suggesting an indirect effect via an OT-induced increase in firing of Type I interneurons. As Type II neurons were shown to project to the central amygdala (CeA), we also recorded from retrogradely labeled *BNST➔CeA* neurons, which we identified as Type II. These results present a model of fine-tuned modulation of intrinsic $BNST_{DL}$ neurocircuitry by OT, which selectively excites Type I neurons, leading to increased GABA-ergic inhibition in Type II projection neurons. Lastly, we demonstrate that fear-conditioning increases sIPSCs frequency in Type II neurons, mimicking the effect of OT. Based on the findings, we propose that OTR in the $BNST_{DL}$ facilitate cued fear by inhibiting *BNST➔CeA* neurons.

1. Introduction

Oxytocin (OT) is a nine amino acid peptide serving as a hypothalamic hormone, which regulates uterine contractions during labor, milk ejection reflex during lactation [1,2], as well as water-electrolyte balance [3,4]. As a neuromodulator in the central nervous system, OT facilitates social behaviors [5–7] and regulates fear and anxiety-like behaviors, for review see [8,9]. Although OT has been shown to modulate fear responses primarily in the central amygdala (CeA) [10–12], we recently showed that oxytocin receptor (OTR) transmission in the dorsolateral bed nucleus of the stria terminalis ($BNST_{DL}$) facilitates the formation of cued fear and improves fear discrimination to signaled vs. un-signaled threats [13,14].

On a cellular level, OT has shown robust modulatory influence on the neurocircuitry of the hippocampus [15–18], auditory cortex [19], ventral tegmental area [20,21], and CeA [10–12,22]. Notably, although the BNST has one of the highest expression levels of OTR in the rodent brain [23–26] and receives OT inputs from hypothalamic nuclei [10,13,23], the effects of OT on excitability and synaptic transmission of BNST neurons are unknown. Studies in the 90's from the Ingram group using electrophysiological approaches have shown that OT increases the spontaneous firing frequency in a subpopulation of BNST neurons in lactating female rats [27–29], but their phenotype is not known.

$BNST_{DL}$ neurons are GABA-ergic [30–32], and functionally connected via a dense intrinsic inhibitory network [33]. As originally described by Rainnie and colleagues, $BNST_{DL}$ neurons can be classified into three major neuron types (I-III) based on their electrophysiological phenotype defined as a unique pattern of voltage deflection in response to transient depolarizing and hyperpolarizing current injections [34,35] and/or based on a single-cell mRNA expression of ion channel subunits [36]. Recently, it was shown that both Type II and Type III are output neurons of the BNST, with major projections to the CeA and lateral hypothalamus, respectively [37].

In the current study, using *in vitro* slice patch-clamp recordings in male Sprague-Dawley rats, we investigated the effects of OT on intrinsic excitability and inhibitory synaptic transmission in Type I-III $BNST_{DL}$ neurons. We show that OT is a powerful modulator of the intrinsic inhibitory network such as it selectively increases the excitability and firing frequency of regular spiking, Type I neurons. As a result of this increased firing of Type I neurons, OT increases inhibitory synaptic transmission selectively in Type II neurons. We also combined injections of a fluorescent retrograde tracer into the CeA with electrophysiological recordings from fluorescent $BNST_{DL}$ neurons and we confirm that the CeA-projecting (*BNST➔CeA*) neurons are identified as Type II. Finally, as we showed before that fear-conditioning evokes OT release in the $BNST_{DL}$ [13], in the current study we also demonstrate that cued fear-conditioning potentiates inhibitory synaptic transmission in Type II $BNST_{DL}$ neurons, and as such mimics the effects of OT.

2. Material and methods

2.1. Animals

Male Sprague-Dawley rats (Envigo, Chicago, IL; 240-300 g) were housed in groups of three on a 12 h light/dark cycle (light 7 a.m. to 7 p.m.) with free access to water and food. Rats were habituated to this environment for one week before the experiments began. Experiments were performed in accordance with the guidelines of the NIH and approved by the Animal Care and Use Committee at RFUMS. A total of 90 rats were used for the experiments. The effects of OT on membrane properties were tested in 14 Type I neurons (from 10 rats), 13 Type II (12 rats), and 9 Type III neurons (8 rats). The effect of OT on firing was tested on 12 Type I (11 rats), 8 Type II (7 rats), and 9 Type III neurons (8 rats). To study the effect of OT on sIPSCs, we recorded 14 Type II (12 rats), 6 Type I (5 rats), and 8 Type III neurons (8 rats). We recorded 6 Type II neurons (4 rats) in experiment with OTR antagonist, and 6 Type II neurons (5 rats) in TTX experiment. To compare sIPSCs between control (4) rats and fear-conditioned (6) rats, we

recorded 11 and 10 neurons, respectively. See **Supplemental Information** for detailed methods.

2.2. Patch-clamp recordings

Rats were anaesthetized with isoflurane USP (Patterson Veterinary, Greeley, CO, USA) before decapitation. Brains were quickly removed and cut into coronal 300 μm slices, and whole-cell patch-clamp recordings were performed from $BNST_{DL}$ neurons as before [38–40]. To study the effects of OT (0.2 μM, based on [21,41], oxytocin acetate salt, # H-2510, Bachem, Switzerland) on intrinsic membrane properties and firing activity, patch pipettes were filled with potassium gluconate internal solution. To study the effects of OT on inhibitory synaptic activity, patch pipettes were filled with high chloride internal solution. To verify that the effects of OT were mediated by OTRs, selective and potent OTR antagonist d(CH2)5(1), D-Tyr(2), Thr(4), Orn(8), des-Gly-NH2(9)]-Vasotocin trifluoroacetate salt [42] (0.4 μM, OTA, V-905 NIMH Chemical Repository) was applied 10 min before OT in all experiments.

2.2.1. The effect of OT on intrinsic membrane properties and firing activity of Type I-III $BNST_{DL}$ neurons

At the beginning of the recording sessions in a current clamp mode, neurons were electrophysiologically characterized into three types (I-III) using current pulses (450 msec in duration) from -350 pA to 80 pA in 5 or 10 pA increments [35]. Next, we investigated the effects of OT on intrinsic membrane properties: resting membrane potential (RMP), input resistance (Rin), rheobase (Rh), threshold of the first action potential (Th) (calculated as the voltage at which the depolarization velocity exceeded 5 mV/ms), and latency of the first spike (Lat) evoked at the Rh current. We also investigated spiking ability by measuring the input-output (I-O) relationship before and after OT application. Steady state frequency (SSF) was measured by applying depolarizing pulses (1 sec in duration) of different amplitudes (0-80 pA in 10 pA increments). We also measured amplitudes of fast, medium and late afterhyperpolarization (fAHP, mAHP and lAHP). As the K^+ currents underlying these AHPs are considered to regulate

excitability and spike frequency adaptation [43,44], we also measured early and late spike frequency adaptation before and after OT application.

2.2.2. The effect of OT on inhibitory synaptic activity of Type I-III $BNST_{DL}$ neurons

To study the effect of OT on spontaneous inhibitory postsynaptic currents (sIPSCs), the events were recorded from Type I-III neurons in a voltage clamp mode at holding potential of -70 mV. To isolate the sIPSCs, the recordings were made in the presence of the AMPA receptor antagonist CNQX (10 μM) and the NMDA receptor antagonist AP-5 (50 μM).

The sIPSCs were characterized by their mean frequency, amplitude, and charge using custom scripts in MatLab. To reach an adequate number of events, the sIPSCs were acquired continuously in 2-minute sweeps during the entire recording time. The sIPSCs were recorded for 10 min in aCSF, followed by 12 min bath application of OT and followed by the drug washout (at least 10 more min after the OT application was completed). As sIPSCs are a combination of spike-independent IPSCs and spike-driven IPSCs, in some experiments the action potential generation was blocked with Tetrodotoxin (TTX, 1 μM, #1078; Tocris Bioscience, UK), leaving only the spike-independent IPSCs. $GABA_A$ receptor antagonist, picrotoxin (25 μM), was used at the end of the recordings to verify the GABA-ergic origin of the sIPSCs.

2.2.3. CeA-projecting $BNST_{DL}$ neurons

To determine an electrophysiological phenotype of *BNST➔CeA* neurons, rats were first bilaterally injected into the CeA with a retrograde tracer, green microbeads (Lumafluor Inc., 100 nl; AP: -2.4 mm, ML: +4.2 mm, DV: -8.2 mm), and were allowed to recover for 4-7 days before electrophysiological recordings. Stereotaxic surgeries were performed as before [13,14]. The slices were illuminated with CoolLED pE-300lite (Scientifica Ltd., Uckfield, UK) and ET - EGFP (FITC/Cy2) filter (Chroma Technology Corp, Bellows Falls, VT, US) to enable visually guided patching of fluorescent neurons. Slices were stored in 10% stabilized formalin post-recordings, mounted with Krystalon Mounting medium (Millipore Sigma, #64969-71), and analyzed with

Nikon Eclipse E600 microscope (Melville, NY, US) and Olympus Fv10i confocal microscope for high magnification imaging (Center Valley, PA, US).

2.2.4. The effect of fear-conditioning on inhibitory synaptic transmission in $BNST_{DL}$ neurons

Cued fear-conditioning was performed as before [13,14]. Briefly, rats were exposed to 10 presentations of a 3.7 s cue light (conditioned stimulus, CS), each co-terminating with a 0.5 s foot shock (unconditioned stimulus, US; 0.5 mA), whereas control rats were placed inside the chamber without presentation of CS or US. 15 min after the end of the session, rats were decapitated and the slice preparation and sIPSCs recordings were performed as above.

2.3. Statistical analysis

All data are presented as MEAN ± standard error of mean (SEM). Distribution of data sets was evaluated with Kolmogorov-Smirnov test. Based on normal distribution, the effects of OT on the sIPSCs, excitability, and firing frequency were analyzed by a repeated measures (RM) one-way analysis of variance (ANOVA) or mixed effects model (when some post-drug time points were missing). Where the F-ratio was significant, all-pairwise post hoc comparisons were made using Tukey's or Sidak's tests. The statistical analyses were completed using GraphPad Prism version 8.0 (GraphPad Software Inc., San Diego, CA). $P \leq 0.05$ was considered significant.

3. Results

3.1. The effects of OT on intrinsic membrane properties and excitability in Type I-III $BNST_{DL}$ neurons.

In Type I neurons, OT induced a significant depolarization of RMP from -62.39 ± 0.84 mV to -57.94 ± 1.39 mV in comparison to baseline (pre, P = 0.0013), as well as in comparison to washout (post, P = 0.0304, **Fig. 1A-B**). This was associated with a significant increase of Rin from 170.98 ± 8.6 MΩ to 233.64 ± 18.6 MΩ (P = 0.0085, **Fig. 1C**). As a consequence, OT induced a significant reduction of Rh from 21.96 ± 2.29 pA to 17.32 ± 2.26 pA (P = 0.0023, **Fig.**

1A, 1D). The Th of the first spike was also significantly reduced from - 38.38 ± 0.68 mV to -39.75 ± 0.88 mV after OT (*P* = 0.0346**, Fig. 1E**). When the selective OTR antagonist (OTA) was applied for 10 min before and during OT application, OT did not significantly affect RMP (*P* = 0.0710), Rh (*P* = 0.1231), Th (*P* = 0.3532) or Lat (*P* = 0.6252, **not shown**).

In addition, OT caused a leftward shift of input/output (I-O) relationship in Type I neurons, demonstrating a significant increment effect on SSF at 40 pA, 50 pA, and 60 pA. Post-hoc test showed a significant increase of the SSF after OT from 6.81 ± 0.68 Hz to 8.96 ± 0.63 Hz in comparison to baseline (pre, *P* = 0.0032) and washout (post, *P* = 0.0095) at 40 pA; from 8.73 ± 0.73 Hz to 11.20 ± 0.70 Hz (*P* = 0.0163, pre and *P* = 0.0226, post) at 50 pA; and from 9.22 ± 0.57 Hz to 11.89 ± 0.99 Hz (*P* = 0.0271, pre and *P* = 0.0054, post) at 60 pA. The OT effect reached a trend at 30 pA (from 5.64 ± 0.5 Hz to 7.31 ± 0.53 Hz, *P* = 0.0820) and at 70 pA (from 10.79 ± 0.6 Hz to 13.62 ± 0.99 Hz, *P* = 0.0794). The effect was not significant at 20 pA (*P* = 0.1268) and 80 pA (*P* = 0.1320, **Fig. 2A-B**). Importantly, in the presence of OTA, OT did not affect the SSF of Type I neurons at 80 pA (*P* = 0.7960), 70 pA (*P* = 0.4237), 60 pA (*P* = 0.6312), 50 pA (*P* = 0.4299), 40 pA (*P* = 0.3365), or 30 pA (*P* = 0.4817, **Fig. 2C**). No spontaneous firing was observed in any type of the $BNST_{DL}$ neurons.

This increase in the spiking ability of Type I neurons after OT was associated with a significant shortening of the first spike's latency from 326.44± 28.63 msec to 224.58 ± 32.51 msec (*P* = 0.0083, **Fig. 1F**). Therefore, we also investigated the effects of OT on three components of the AHP (fAHP, mAHP, lAHP) in Type I neurons. OT significantly reduced the amplitude of fAHP (from 8.63 ± 0.89 mV to 7.47 ± 0.77 mV, *P* = 0.0062, **Fig. 3A-B**) and mAHP (from 10.69 ± 0.61 mV to 8.45 ± 0.72 mV, *P* = 0.0001, pre and *P* = 0.0003, post), **Fig. 3A, D**). Notably, OT did not affect amplitudes of fAHP (*P* = 0.2220, **Fig. 3C**) and mAHP (*P* = 0.3968, **Fig. 3E**) in the presence of OTA. Lastly, OT did not significantly affect the amplitude of lAHP (*P* = 0.2401, **not shown**).

We also investigated if these changes in AHP amplitude could modify early and late spike frequency adaptation. We found that OT significantly increased the instantaneous frequency of ISIs and post-hoc test showed a significant OT effect on frequency (in Hz) of ISI number 2 (ISI-2) from 16.77 ± 1.55 to 19.57 ± 1.2 (P = 0.0006), ISI-3 from 12.48 ± 0.88 to 16.19 ± 1.09 (P < 0.0001), ISI-4 from 11.92 ± 0.88 to 14.87 ± 0.76 (P = 0.0006), ISI-5 from 11.36 ± 0.68 to 14.58 ± 0.77 (P = 0.0001), ISI-6 from 11.26 ± 0.72 to 13.93 ± 0.76 (P = 0.0079), and ISI-7 from 10.58 ± 0.64 o 13.44 ± 0.88 (P = 0.0051, **Fig. 3F**).

In contrast to Type I neurons, OT did not affect the intrinsic membrane properties or the firing properties of Type II and III neurons (**Supplementary Table 1**). OT also did not affect SSF in Type II and Type III neurons (**Fig. 2D-E**). Overall, these results suggest that OT increases the excitability and facilitates the firing selectively in Type I $BNST_{DL}$ neurons in an OTR-dependent manner.

3.1. The effects of OT on inhibitory synaptic transmission in Type I-III $BNST_{DL}$ neurons.

In Type II $BNST_{DL}$ neurons, application of OT caused a significant increase in the frequency of sIPSCs in 12 out of 14 recorded neurons from 1.03 ± 0.20 Hz to 2.64 ± 0.47 Hz in comparison to baseline (pre, P = 0.0033), and in comparison to washout (post, P = 0.0018, **Fig. 4A-B**). Notably, the effect of OT on the sIPSCs frequency was not associated with a significant change in the amplitude (P = 0.9205, **Fig. 4C**) or in the total charge (P = 0.5744, **not shown**). In addition, when the spike-driven sIPSCs were blocked with TTX (P = 0.0387), OT no longer affected the frequency of sIPSCs of Type II neurons (P = 0.9975, **Fig. 4D**). OT did not increase the sIPSCs frequency in the presence of OTA (P = 0.3053**, Fig. 4E**). These results demonstrate that OT increases the frequency of spike-driven sIPSCs selectively in Type II neurons.

In Type I neurons, OT did not affect the sIPSCs frequency (P = 0.3018), amplitude (P = 0.3347), or total charge (P = 0.6087, **not shown**). In Type III neurons, OT did not affect the frequency (P = 0.9440, **Fig. 4F**), but it reduced amplitude (P = 0.0314, **Fig. 4G**) and total charge of IPSCs (P = 0.0372).

3.3. CeA-projecting $BNST_{DL}$ neurons

In rats injected with microbeads into the CeA, retro-labeled fluorescent neurons were found in subdivisions of the $BNST_{DL}$, primarily in the oval nucleus of the $BNST_{DL}$ ($BNST_{OV}$) and to a lesser extent in anteromedial BNST ($BNST_{AM}$, **Fig. 5A-B**). We found healthy fluorescent neurons that were suitable for recordings in 6 out of 17 rats. In the slices from those 6 rats, we recorded 8 fluorescent neurons (**Fig. 5C**) and all of them were classified as Type II neurons (**Fig. 5D**).

3.4. The effect of fear-conditioning on sIPSCs in $BNST_{DL}$ neurons

In Type II neurons, the sIPSCs frequency was significantly increased in fear-conditioned rats (3.54 ± 0.52 Hz) respective to controls (1.74 ± 0.35 Hz, unpaired *t*-test, $P = 0.0131$). This increase in frequency was not associated with significant changes in amplitude or sIPSCs charge ($P = 0.4384$ and $P = 0.3924$, respectively, **Fig. 5E-F**).

4. Discussion

Here we demonstrate that OT regulates the intrinsic inhibitory network of the $BNST_{DL}$, where it increases firing of Type I, regular spiking neurons, and potentiates GABA-ergic inhibition in Type II, burst firing neurons. Using visually guided patching of retro-labeled $BNST_{DL}$ neurons, we confirm that Type II are output neurons of the $BNST_{DL}$, which project to the CeA (*BNST➔CeA* neurons). Therefore, we demonstrate that there are two groups of OT-responsive neurons in the $BNST_{DL}$; a population of interneurons (Type I) that is directly excited by OTR activation, and a group of output neurons (Type II) that demonstrates increased synaptic inhibition after OT application (see **Fig. 5G).** We also show that cued fear-conditioning modulates synaptic transmission of the $BNST_{DL}$ and increases GABA-ergic inhibition in Type II neurons, mimicking the effect of OT. The OT-mediated inhibition of the $BNST_{DL}$ output has powerful implications for the modulation of fear and anxiety-like behaviors.

Neurons of the $BNST_{DL}$ are GABA-ergic [30,32,38] and can be categorized into three major types (I-III) [34,35]. Type I neurons, which are characterized by regular firing and lack of

burst-firing activity [35,36], were classified as interneurons by Paré and colleagues [45]. We show that Type I neurons are the primary OT-responsive neurons of the $BNST_{DL}$ as demonstrated by their increased excitability and firing rate after OT application. Previous studies using single unit recordings showed that OT increased the spontaneous firing rate of 50% of BNST neurons in lactating female rats [28], and the magnitude of the response was significantly potentiated during lactation [27]. In our study, the OT effects on Type I neurons are paralleled by increased inhibitory transmission observed selectively in Type II neurons. The specific effect of OT on the sIPSCs frequency, but not amplitude, indicates a presynaptic effect in Type II neurons. More importantly, the OT effect in Type II neurons was no longer observed when the spike-driven IPSCs were suppressed with TTX, indicating that the influence is indirect and driven by increased firing of $BNST_{DL}$ interneurons. These results suggest that Type I neurons are indeed interneurons providing inhibitory synaptic input to Type II neurons, an effect potentiated by OT.

In contrast, in Type III neurons, we observed reduced amplitude and total charge, but not frequency of sIPSC after OT application, indicating a postsynaptic effect. OT was shown previously to depress GABA-ergic synapses in supraoptic nucleus of the hypothalamus via postsynaptic mechanism [46]. However, since in our hands the effect on the amplitude was accompanied by a reduction in the total charge, this could potentially indicate shortening of GABA channel opening via OTR-mediated increases in intracellular Ca^{2+}, as demonstrated after OTR activation before [47]. The effect of OT on sIPSC amplitude in Type III neurons needs to be interpreted with caution and explored more in the future studies.

To further investigate the OT effects on intrinsic excitability and firing, we demonstrated that OT reduced fAHP and mAHP selectively in Type I neurons. AHPs generated after a single action potential or a train of action potentials limit the frequency of neuronal firing [46], as demonstrated by a significant increase in action potential firing after pharmacological inhibition of AHPs [47]. The fAHP, mediated by BK channels, is responsible for early spike frequency

adaptation in many neuronal types [44]. The mAHP is mediated by the non-inactivating M-current, which blockade with selective antagonist reduces late spike adaptation [48,49]. An OTR-mediated increase of neuronal excitability was recently shown in the hippocampus, where a selective OTR agonist induced membrane depolarization and increased membrane resistance in CA2 pyramidal cells leading to a leftward shift in their firing frequency-current relationship [50]. Here we show that OT-mediated excitation of Type I neurons in the $BNST_{DL}$ was associated with a significant increase in instantaneous frequency of action potentials due to the reduction in the early and late adaptation. In combination with the OT effect on intrinsic membrane properties, this could explain the increased firing frequency observed in Type I neurons. In order to investigate the effects of OT on intrinsic excitability, the recordings were performed in the presence of GABA-ergic and glutamatergic blockers. As a result of this, combined with a mostly de-afferented BNST, there was no spontaneous firing observed in Type I-III neurons (without a current injection). In fact, spontaneous firing is rarely observed during patch-clamp recordings [51]. However, we cannot rule out that these neurons fire spontaneously *in vivo* and that OT would increase spontaneous firing rate in Type I neurons in these conditions.

Similar modulation of the intrinsic inhibitory network by OT was shown in a variety of brain regions. In the CeA, there are also two groups of OT-responsive neurons. A group of interneurons located in the lateral CeA (CeL) [52] is excited by OTR activation [11,53]. Once excited by OT, these interneurons provide inhibitory input to medial CeA (CeM) output neurons, which project to lateral periaqueductal gray and reduce contextual fear [12], for review see [54]. Similarly, in the hippocampus [15–18,55], lateral amygdala [41], and the prefrontal cortex [19,56], OT was shown to excite a population of interneurons, usually fast-spiking parvalbumin interneurons, which then inhibit glutamatergic projection neurons.

It is important to note that the BNST also contains neurons producing arginine-vasopressin **(**AVP) [57] and has a high expression of AVP receptors, V1AR [58]. As OT shows a relatively high affinity toward AV1R, this raises a possibility of non-specific effects via V1AR.

However, the OT effects in our study were all blocked by OTA, which is highly selective toward OTR with a negligible affinity toward V1AR, see Table 8 in [42]**.** In addition, the BNST was not entirely isolated during recordings, such as the slice also contained GABA-ergic neurons in the medial preoptic area, MPA [59], which express OTR [60], and project to the BNST [61]. However, this projection reaches primarily the principal encapsulated nucleus in the posterior BNST [62], where OTR are involved in reproductive behavior [63]. Notably, the posterior BNST is not a part of our slice preparation.

Previously, using *in vivo* microdialysis in awake rats, we have shown that cued fear-conditioning evokes OT release in the $BNST_{DL}$ [13]. Therefore, fear-conditioning could mimic, at least to some extent, OT effects in the $BNST_{DL}$. Here, we demonstrate that cued fear-conditioning increases inhibitory synaptic transmission in Type II $BNST_{DL}$ neurons, mimicking the effect of OT. These results provide a functional relevance for the OT modulation of $BNST_{DL}$ activity in a context of fear learning. In fact, previous studies using *in vivo* single unit recordings have shown a bi-directional effect of fear-conditioning on BNST neurons, where 10% of recorded neurons acquire excitatory responses, whereas inhibitory responses emerge in 20% of the recorded neurons [64]. The ON neurons identified in the study might potentially correspond to Type I neurons, which are excited by OT. The OFF neurons, on the other hand, might correspond to Type II neurons, which demonstrate increased GABA-ergic inhibition after OT application and we have shown the same inhibition pattern after fear-conditioning. These results confirm that the $BNST_{DL}$ neurons are recruited during fear-conditioning and they show a similar pattern of excitation/inhibition between fear-conditioning and application of OT. More recent electrophysiological recordings during fear acquisition also revealed two subpopulations of BNST neurons in which their firing patterns predicted fear responses during retrieval [65].

Notably, Type II neurons are the most abundant and heterogeneous neuronal population in the rat $BNST_{DL}$ [66,67] and they were recently identified as output neurons of the $BNST_{DL}$ with 60% of them projecting to the CeA [37]. Therefore, we also recorded from the *BNST➔CeA* neurons and confirmed that all retrogradely labeled BNST neurons belong to the Type II

classification. A functional inhibitory projection from the BNST to the CeA has been demonstrated using optogenetics [67,68]. The BNST is known to mediate anxiety [31,69–71], contextual fear [70,72,73], as well as fear responses to un-signaled, diffuse, or unpredictable threats [74–76]. A recent optogenetic study showed that activation of the *BNST➔CeA* projection increases anxiety-like behavior [37], suggesting that the *BNST➔CeA* neurons are important output neurons in mediating anxiety. In addition, the BNST has been shown to inhibit cued fear responses to discrete threats [77]. However, our recent behavioral studies demonstrate that OTR transmission in the $BNST_{DL}$ facilitates acquisition of cued fear and reduces fear responses to un-signaled/diffuse threats [8,13,14], showing opposite effects to the BNST activation. Therefore, based on the current electrophysiology results, we conclude that by increasing firing of Type I neurons and strengthening GABA-ergic input in Type II neurons, OT inhibits the *BNST➔CeA* projection neurons. Thus, we propose that OTR transmission in the $BNST_{DL}$ facilitates cued fear and reduces anxiety by inhibiting the *BNST➔CeA* output.

5. Acknowledgements

We would like to thank Dr. Attilio Caravelli for his help with Matlab. We also thank Rachel Chudoba for proofreading the manuscript. This work was supported by grant from the National Institute of Mental Health R01 MH113007 to JD and start-up funds from the Chicago Medical School, Rosalind Franklin University of Medicine and Science to JD.

6. Contributions

JD and WF designed the study. WF, FB, and VO acquired data. WF, FB, VO, and JD analyzed data. WF, FB, VO and JD interpreted data. WF and JD wrote the manuscript. JD obtained funding.

7. Financial Disclosures

The authors declare no conflict of interest and have no financial interests to disclose. Dr. Joanna Dabrowska reports submission of a provisional patent application entitled: Method and

System for Testing for Stress-related Mental Disorders, Susceptibility, Disease Progression, Disease Modulation and Treatment Efficacy (# 62/673447).

8. Figure legends

Figure 1. Oxytocin affects intrinsic membrane properties of Type I $BNST_{DL}$ neurons. A: A representative trace showing that oxytocin (OT, 0.2 μM) shortens the latency to the 1st spike at rheobase current (Rh) and depolarizes resting membrane potential (RMP, from -64 mV to -60 mV). This is associated with increased input resistance (Rin), measured with a depolarizing current step below the Rh. OT also reduces Rh from 30 pA (pre) to 20 pA (OT) **B-D**: Line graphs with individual neurons' responses (gray) showing that OT significantly increases the RMP (**B**, P = 0.0002, F (1.593, 19.12) = 15.76, n = 14, mixed-effect analysis), increases Rin (**C**, P = 0.0085, n = 9, paired *t*-test), reduces the Rh (**D**, P = 0.0457, F (1.341, 16.09) = 4.226, n = 14, mixed-effect analysis), reduces the 1st spike threshold (**E**, P = 0.0164, F (1.472, 20.61) = 5.749, and reduced the 1st spike latency (**F**, P = 0.0185, F (1.971, 23.66) = 4.775, n = 14, mixed-effect analysis). Thick black lines show average responses for all Type I neurons recorded. Each data point represents the mean ± SEM, **P < 0.01, *P < 0.05 in comparison to pre or post-OT.

Figure 2. Oxytocin increases intrinsic excitability of Type I, but not Type II or Type III, $BNST_{DL}$ neurons. **A**: A representative trace showing voltage deflections in response to hyperpolarizing and depolarizing current injections characteristic of Type I neuron (left) and the increase in firing frequency of Type I neuron in the presence of OT respective to baseline (pre) (right). **B**: OT causes a leftward shift of input/output (I-O) relationship in Type I neurons. The steady state frequency (SSF) was determined as an average of an inverse of the inter-spike intervals (ISI) from all action potentials starting from the second action potential. In Type I neurons***,*** OT shows a significant increment effect on SSF at 40 pA (P = 0.0024, F (1.667, 15.01) = 10.11), at 50 pA (P = 0.0271, F (1.863, 16.76) = 4.628), and at 60 pA (P = 0.0271, F (1.688, 11.82) = 5.267, mixed-effects analysis). **C**: Application of OTR antagonist, OTA (0.4 μM),

prevents the leftward shift of the I-O relationship induced by OT application (40 pA, P = 0.3365, 50 pA, P = 0.4299, 60 pA, P = 0.6312, n = 5, RM ANOVA). **D-E:** OT application does not modify the I-O relationship in Type II (**D**) or Type III $BNST_{DL}$ neurons (**E**). In Type II neurons, OT did not affect SSF at 80 pA (P = 0.3116), 70 pA (P = 0.8236), 60 pA (P = 0.9519), 50 pA (P = 0.8993), 40 pA (P = 0.7636), 30 pA (P = 0.8673), or at 20 pA (P = 0.6990, **D**). Similarly, in Type III neurons, there was no effect of OT on SSF at 80 pA (P = 0.1151), 70 pA (P = 0.1138), 60 pA (P = 0.180), 50 pA (P = 0.0847), 40 pA (P = 0.1041), 30 pA (P = 0.0790), or at 20 pA (P = 0.0681, **E**). Each data point represents the mean ± SEM, **P < 0.01, *P < 0.05 in comparison to pre-OT, ## P < 0.01, # P < 0.05 in comparison to post-OT.

Figure 3. Oxytocin reduces fast and medium afterhyperpolarizations and modifies early and late spike frequency adaptation in Type I $BNST_{DL}$ neurons. **A**: A representative trace from Type I neuron showing a reduction of fast AHP (fAHP) and medium AHP (mAHP) after OT application respective to baseline (pre). The amplitudes of the fAHP and mAHP following the first action potential evoked at Rh were calculated as the difference from the action potential threshold to the membrane voltage measured after 2-5 msec and 50-100 msec, respectively. The lAHP was measured at 2000 msec after the end of the depolarizing pulse, following generation of five action potentials. **B**: Line graphs showing individual neurons' responses (gray) and reduction of the fAHP during OT application (P = 0.0124, F (1.473, 17.68 = 6.493, mixed-effects analysis, n = 14). **C**: OTR antagonist, OTA (0.4 μM), prevents the OT-induced reduction of fAHP (P = 0.2220, n = 7, RM one-way ANOVA). **D**: Line graph showing reduction of mAHP during OT application (P <0.0001, F (1.844, 22.13) = 23.25, mixed effect analysis, n = 14). **E***:* OT-induced reduction of mAHP is blocked by OTR antagonist, OTA (P = 0.3968, n = 7, RM one-way ANOVA). Thick black lines show average responses for all Type I neurons recorded. **F**: OT modifies early and late spike frequency adaptation. The early and late spike frequency adaptation was investigated using a depolarizing pulse of 1 sec and measuring the instantaneous frequency for every action potential interval. The ISI number is the inter-stimulus interval between two consecutive action potentials. OT significantly increased the instantaneous

frequency of ISI (P < 0.0001, F (1, 13) = 82.69, mixed effects model). Each data point represents the mean ± SEM, ****P < 0.0001, ***P < 0.001, **P < 0.01, *P < 0.05.

Figure 4. Oxytocin modulates inhibitory synaptic transmission in $BNST_{DL}$ neurons. A: Representative recordings showing an increase in the frequency of spontaneous inhibitory postsynaptic currents (sIPSCs) after OT application respective to baseline (pre). **B-C**: Line graphs (gray) showing that 12 out of 14 recorded Type II neurons showed an increase in sIPSCs frequency (**B**, P = 0.0022, F (1.058, 12.17) = 14.41, n = 14, mixed-effect analysis) but not amplitude (**C**, P = 0.5855, F (1.563, 17.19) = 0.4718, n = 14, mixed-effect analysis) after OT application. **D**: OT does not affect sIPSC frequency in a presence of OTR antagonist, OTA (0.4 μM) (P = 0.1788, F (1.469, 8.814) = 2.135, n = 6, RM ANOVA). **E**: When spike-driven IPSCs were blocked with TTX (P = 0.0151, F (1.030, 6.179) = 10.98, n = 6, RM ANOVA), OT does not affect the sIPSCs frequency. **F-G**: OT does not affect frequency (**F**, P = 0.9362) but reduces amplitude of sIPCS in Type III neurons (**G**, P = 0.0160, paired *t*-test). Thick black lines show averaged responses for all neurons recorded. Each data point represents the mean ± SEM, **P < 0.01, *P < 0.05 in comparison to pre- or post-OT.

Figure 5. Type II neurons are output neurons of the $BNST_{DL}$ to the central amygdala and demonstrate increased inhibitory transmission after fear-conditioning. A-B: Microphotographs showing neurons expressing green fluorescent microbeads in the $BNST_{DL}$ after the retro-beads were injected into the central amygdala (CeA). **A**: BNST neurons projecting to the CeA (*BNST➔CeA* neurons) were primarily found in the dorsolateral BNST, primarily the oval nucleus, and to a lesser extent in the anteromedial BNST (20x, LV – Lateral ventricle, IC – Internal capsulae, $BNST_{AM}$ - anteriomedial BNST, $BNST_{OV}$ - oval nucleus of the BNST, scale bar 100 μm). **B**: High magnification (60x) microphotographs showing green fluorescent beads present in membranes and processes of the *BNST➔CeA* neurons (scale bar 10 μm). **C-D**: Electrophysiological characterization of the *BNST➔CeA* neurons using visually guided patching (**C**, 40x, scale bar 20 μm). Representative recording of the BNST➔CeA

fluorescent neuron showing the electrophysiological properties of a Type II neuron such as the presence of a sag during the hyperpolarized current pulses and the spike rebound at the end of the 450 ms current pulse injection (**D**). **E-F**: Bar graphs showing that cued fear-conditioning increases inhibitory synaptic transmission in Type II neurons, such as sIPSCs frequency was significantly increased in fear-conditioned rats respective to controls (unpaired *t*-test, P = 0.0131). This increase in sIPSCs frequency was not associated with significant changes in sIPSCs amplitude (P = 0.4384). **G**: Diagram showing that OT regulates the intrinsic inhibitory network and output neurons of the $BNST_{DL}$. By increasing firing frequency of Type I regular spiking neurons, OT potentiates GABA-ergic inhibition on Type II $BNST_{DL}$ neurons. Type II neurons are output neurons of the $BNST_{DL}$ sending projections to the central amygdala CeA (*BNST➔CeA* neurons*)*. Hence, OT modulates intrinsic excitability in the $BNST_{DL}$ neurocircuitry and it can also inhibit the *BNST➔CeA* output neurons.

9. References

1. Caldeyro-Barcia R, Poseiro JJ. Oxytocin and contractility of the pregnant human uterus. Ann N Y Acad Sci. 1959;75:813–830.
2. Nickerson K, Bonsness RW, Douglas RG, Condliffe P, Du Vigneaud V. Oxytocin and milk ejection. Am J Obstet Gynecol. 1954;67:1028–1034.
3. Han JS, Maeda Y, Knepper MA. Dual actions of vasopressin and oxytocin in regulation of water permeability in terminal collecting duct. Am J Physiol. 1993;265:F26-34.
4. Verbalis JG, Blackburn RE, Olson BR, Stricker EM. Central oxytocin inhibition of food and salt ingestion: a mechanism for intake regulation of solute homeostasis. Regul Pept. 1993;45:149–154.
5. Bosch OJ, Young LJ. Oxytocin and Social Relationships: From Attachment to Bond Disruption. Curr Top Behav Neurosci. 2018;35:97–117.
6. Pedersen CA, Caldwell JD, Peterson G, Walker CH, Mason GA. Oxytocin activation of maternal behavior in the rat. Ann N Y Acad Sci. 1992;652:58–69.
7. Tabbaa M, Paedae B, Liu Y, Wang Z. Neuropeptide Regulation of Social Attachment: The Prairie Vole Model. Compr Physiol. 2016;7:81–104.
8. Janeček M, Dabrowska J. Oxytocin facilitates adaptive fear and attenuates anxiety responses in animal models and human studies-potential interaction with the corticotropin-

releasing factor (CRF) system in the bed nucleus of the stria terminalis (BNST). Cell Tissue Res. 2019;375:143–172.

9. Neumann ID, Slattery DA. Oxytocin in General Anxiety and Social Fear: A Translational Approach. Biol Psychiatry. 2016;79:213–221.
10. Knobloch HS, Charlet A, Hoffmann LC, Eliava M, Khrulev S, Cetin AH, et al. Evoked axonal oxytocin release in the central amygdala attenuates fear response. Neuron. 2012;73:553–566.
11. Terburg D, Scheggia D, Triana Del Rio R, Klumpers F, Ciobanu AC, Morgan B, et al. The Basolateral Amygdala Is Essential for Rapid Escape: A Human and Rodent Study. Cell. 2018;175:723-735.e16.
12. Viviani D, Charlet A, van den Burg E, Robinet C, Hurni N, Abatis M, et al. Oxytocin selectively gates fear responses through distinct outputs from the central amygdala. Science. 2011;333:104–107.
13. Martinon D, Lis P, Roman AN, Tornesi P, Applebey SV, Buechner G, et al. Oxytocin receptors in the dorsolateral bed nucleus of the stria terminalis (BNST) bias fear learning toward temporally predictable cued fear. Transl Psychiatry. 2019;9:140.
14. Moaddab M, Dabrowska J. Oxytocin receptor neurotransmission in the dorsolateral bed nucleus of the stria terminalis facilitates the acquisition of cued fear in the fear-potentiated startle paradigm in rats. Neuropharmacology. 2017;121:130–139.
15. Harden SW, Frazier CJ. Oxytocin depolarizes fast-spiking hilar interneurons and induces GABA release onto mossy cells of the rat dentate gyrus. Hippocampus. 2016;26:1124–1139.
16. Maniezzi C, Talpo F, Spaiardi P, Toselli M, Biella G. Oxytocin Increases Phasic and Tonic GABAergic Transmission in CA1 Region of Mouse Hippocampus. Front Cell Neurosci. 2019;13:178.
18. Owen SF, Tuncdemir SN, Bader PL, Tirko NN, Fishell G, Tsien RW. Oxytocin enhances hippocampal spike transmission by modulating fast-spiking interneurons. Nature. 2013;500:458–462.
19. Marlin BJ, Mitre M, D'amour JA, Chao MV, Froemke RC. Oxytocin enables maternal behaviour by balancing cortical inhibition. Nature. 2015;520:499–504.
20. Hung LW, Neuner S, Polepalli JS, Beier KT, Wright M, Walsh JJ, et al. Gating of social reward by oxytocin in the ventral tegmental area. Science. 2017;357:1406–1411.
21. Xiao L, Priest MF, Nasenbeny J, Lu T, Kozorovitskiy Y. Biased Oxytocinergic Modulation of Midbrain Dopamine Systems. Neuron. 2017;95:368-384.e5.
22. Huber D, Veinante P, Stoop R. Vasopressin and oxytocin excite distinct neuronal populations in the central amygdala. Science. 2005;308:245–248.

23. Dabrowska J, Hazra R, Ahern TH, Guo J-D, McDonald AJ, Mascagni F, et al. Neuroanatomical evidence for reciprocal regulation of the corticotrophin-releasing factor and oxytocin systems in the hypothalamus and the bed nucleus of the stria terminalis of the rat: Implications for balancing stress and affect. Psychoneuroendocrinology. 2011;36:1312–1326.
24. Dumais KM, Bredewold R, Mayer TE, Veenema AH. Sex differences in oxytocin receptor binding in forebrain regions: correlations with social interest in brain region- and sex-specific ways. Horm Behav. 2013;64:693–701.
25. Tribollet E, Dubois-Dauphin M, Dreifuss JJ, Barberis C, Jard S. Oxytocin receptors in the central nervous system. Distribution, development, and species differences. Ann N Y Acad Sci. 1992;652:29–38.
26. Veinante P, Freund-Mercier MJ. Distribution of oxytocin- and vasopressin-binding sites in the rat extended amygdala: a histoautoradiographic study. J Comp Neurol. 1997;383:305–325.
27. Ingram CD, Moos F. Oxytocin-containing pathway to the bed nuclei of the stria terminalis of the lactating rat brain: immunocytochemical and in vitro electrophysiological evidence. Neuroscience. 1992;47:439–452.
28. Ingram CD, Cutler KL, Wakerley JB. Oxytocin excites neurones in the bed nucleus of the stria terminalis of the lactating rat in vitro. Brain Res. 1990;527:167–170.
29. Wilson BC, Terenzi MG, Ingram CD. Differential excitatory responses to oxytocin in sub-divisions of the bed nuclei of the stria terminalis. Neuropeptides. 2005;39:403–407.
30. Cullinan WE, Herman JP, Watson SJ. Ventral subicular interaction with the hypothalamic paraventricular nucleus: evidence for a relay in the bed nucleus of the stria terminalis. J Comp Neurol. 1993;332:1–20.
31. Dabrowska J, Hazra R, Guo J-D, Dewitt S, Rainnie DG. Central CRF neurons are not created equal: phenotypic differences in CRF-containing neurons of the rat paraventricular hypothalamus and the bed nucleus of the stria terminalis. Front Neurosci. 2013;7:156.
32. Sun N, Cassell MD. Intrinsic GABAergic neurons in the rat central extended amygdala. J Comp Neurol. 1993;330:381–404.
33. Xu X, Ikrar T, Sun Y, Santos R, Holmes TC, Francesconi W, et al. High-resolution and cell-type-specific photostimulation mapping shows weak excitatory vs. strong inhibitory inputs in the bed nucleus of the stria terminalis. J Neurophysiol. 2016;115:3204–3216.
34. Daniel SE, Guo J, Rainnie DG. A comparative analysis of the physiological properties of neurons in the anterolateral bed nucleus of the stria terminalis in the Mus musculus, Rattus norvegicus, and Macaca mulatta. J Comp Neurol. 2017;525:2235–2248.

35. Hammack SE, Mania I, Rainnie DG. Differential expression of intrinsic membrane currents in defined cell types of the anterolateral bed nucleus of the stria terminalis. J Neurophysiol. 2007;98:638–656.
36. Hazra, R., Guo, J.-D., Ryan, S.J., Jasnow, A.M., Dabrowska, J., and Rainnie, D.G. (2011b). A transcriptomic analysis of type I-III neurons in the bed nucleus of the stria terminalis. Mol. Cell. Neurosci. *46*, 699–709.
37. Yamauchi, N., Takahashi, D., Sugimura, Y.K., Kato, F., Amano, T., and Minami, M. (2018c). Activation of the neural pathway from the dorsolateral bed nucleus of the stria terminalis to the central amygdala induces anxiety-like behaviors. Eur. J. Neurosci. *48*, 3052–3061.
38. Dabrowska J, Hazra R, Guo J-D, Dewitt S, Rainnie DG. Central CRF neurons are not created equal: phenotypic differences in CRF-containing neurons of the rat paraventricular hypothalamus and the bed nucleus of the stria terminalis. Front Neurosci. 2013;7:156.
39. Dabrowska J, Hazra R, Guo J-D, Li C, Dewitt S, Xu J, et al. Striatal-enriched protein tyrosine phosphatase-STEPs toward understanding chronic stress-induced activation of corticotrophin releasing factor neurons in the rat bed nucleus of the stria terminalis. Biol Psychiatry. 2013;74:817–826.
40. Francesconi W, Berton F, Repunte-Canonigo V, Hagihara K, Thurbon D, Lekic D, et al. Protracted withdrawal from alcohol and drugs of abuse impairs long-term potentiation of intrinsic excitability in the juxtacapsular bed nucleus of the stria terminalis. J Neurosci. 2009;29:5389–5401.
41. Crane JW, Holmes NM, Fam J, Westbrook RF, Delaney AJ. Oxytocin increases inhibitory synaptic transmission and blocks development of long-term potentiation in the lateral amygdala. J Neurophysiol. 2020;123:587–599.
42. Manning M, Misicka A, Olma A, Bankowski K, Stoev S, Chini B, et al. Oxytocin and vasopressin agonists and antagonists as research tools and potential therapeutics. J Neuroendocrinol. 2012;24:609–628.
43. Lopez de Armentia M, Sah P. Firing properties and connectivity of neurons in the rat lateral central nucleus of the amygdala. J Neurophysiol. 2004;92:1285–1294.
44. Gu N, Vervaeke K, Storm JF. BK potassium channels facilitate high-frequency firing and cause early spike frequency adaptation in rat CA1 hippocampal pyramidal cells. J Physiol (Lond). 2007;580:859–882.
45. Rodríguez-Sierra OE, Turesson HK, Pare D. Contrasting distribution of physiological cell types in different regions of the bed nucleus of the stria terminalis. J Neurophysiol. 2013;110:2037–2049.

46. Alger BE, Nicoll RA. Epileptiform burst afterhyperolarization: calcium-dependent potassium potential in hippocampal CA1 pyramidal cells. Science. 1980;210:1122–1124.
47. Pedarzani P, Storm JF. PKA mediates the effects of monoamine transmitters on the K+ current underlying the slow spike frequency adaptation in hippocampal neurons. Neuron. 1993;11:1023–1035.
48. Gu N, Vervaeke K, Hu H, Storm JF. Kv7/KCNQ/M and HCN/h, but not KCa2/SK channels, contribute to the somatic medium after-hyperpolarization and excitability control in CA1 hippocampal pyramidal cells. J Physiol (Lond). 2005;566:689–715.
49. Gu N, Hu H, Vervaeke K, Storm JF. SK (KCa2) channels do not control somatic excitability in CA1 pyramidal neurons but can be activated by dendritic excitatory synapses and regulate their impact. J Neurophysiol. 2008;100:2589–2604.
50. Tirko NN, Eyring KW, Carcea I, Mitre M, Chao MV, Froemke RC, et al. Oxytocin Transforms Firing Mode of CA2 Hippocampal Neurons. Neuron. 2018;100:593-608.e3.
51. Perkins KL. Cell-attached voltage-clamp and current-clamp recording and stimulation techniques in brain slices. J Neurosci Methods. 2006;154:1–18.
52. Gozzi A, Jain A, Giovannelli A, Giovanelli A, Bertollini C, Crestan V, et al. A neural switch for active and passive fear. Neuron. 2010;67:656–666.
53. Haubensak W, Kunwar PS, Cai H, Ciocchi S, Wall NR, Ponnusamy R, et al. Genetic dissection of an amygdala microcircuit that gates conditioned fear. Nature. 2010;468:270–276.
54. Beyeler A, Dabrowska J. Neuronal diversity of the amygdala and the bed nucleus of the stria terminalis. Handbook of Amygdala Structure and Function, vol. 26, London: Academic Press/Elsevier; 2020. p. In press.
55. Zaninetti M, Raggenbass M. Oxytocin receptor agonists enhance inhibitory synaptic transmission in the rat hippocampus by activating interneurons in stratum pyramidale. Eur J Neurosci. 2000;12:3975–3984.
56. Nakajima M, Görlich A, Heintz N. Oxytocin modulates female sociosexual behavior through a specific class of prefrontal cortical interneurons. Cell. 2014;159:295–305.
57. al-Shamma HA, De Vries GJ. Neurogenesis of the sexually dimorphic vasopressin cells of the bed nucleus of the stria terminalis and amygdala of rats. J Neurobiol. 1996;29:91–98.
58. Grundwald NJ, Benítez DP, Brunton PJ. Sex-Dependent Effects of Prenatal Stress on Social Memory in Rats: A Role for Differential Expression of Central Vasopressin-1a Receptors. J Neuroendocrinol. 2016;28.
59. Okamura H, Abitbol M, Julien JF, Dumas S, Bérod A, Geffard M, et al. Neurons containing messenger RNA encoding glutamate decarboxylase in rat hypothalamus demonstrated by in situ hybridization, with special emphasis on cell groups in medial preoptic area, anterior

hypothalamic area and dorsomedial hypothalamic nucleus. Neuroscience. 1990;39:675–699.

60. Sharma K, LeBlanc R, Haque M, Nishimori K, Reid MM, Teruyama R. Sexually dimorphic oxytocin receptor-expressing neurons in the preoptic area of the mouse brain. PLoS ONE. 2019;14:e0219784.
61. Simerly RB, Swanson LW. Projections of the medial preoptic nucleus: a Phaseolus vulgaris leucoagglutinin anterograde tract-tracing study in the rat. J Comp Neurol. 1988;270:209–242.
62. Maejima S, Ohishi N, Yamaguchi S, Tsukahara S. A neural connection between the central part of the medial preoptic nucleus and the bed nucleus of the stria terminalis to regulate sexual behavior in male rats. Neurosci Lett. 2015;606:66–71.
63. Kremarik P, Freund-Mercier MJ, Stoeckel ME. Autoradiographic detection of oxytocin- and vasopressin-binding sites in various subnuclei of the bed nucleus of the stria terminalis in the rat. Effects of functional and experimental sexual steroid variations. J Neuroendocrinol. 1991;3:689–698.
64. Haufler D, Nagy FZ, Pare D. Neuronal correlates of fear conditioning in the bed nucleus of the stria terminalis. Learn Mem. 2013;20:633–641.
65. Bjorni M, Rovero NG, Yang ER, Holmes A, Halladay LR. Phasic signaling in the bed nucleus of the stria terminalis during fear learning predicts within- and across-session cued fear expression. Learn Mem. 2020;27:83–90.
66. Hazra R, Guo J-D, Ryan SJ, Jasnow AM, Dabrowska J, Rainnie DG. A transcriptomic analysis of type I-III neurons in the bed nucleus of the stria terminalis. Mol Cell Neurosci. 2011;46:699–709.
68. Gungor NZ, Yamamoto R, Paré D. Optogenetic study of the projections from the bed nucleus of the stria terminalis to the central amygdala. J Neurophysiol. 2015;114:2903–2911.
69. Daniel SE, Rainnie DG. Stress Modulation of Opposing Circuits in the Bed Nucleus of the Stria Terminalis. Neuropsychopharmacology. 2016;41:103–125.
70. Davis M, Walker DL, Miles L, Grillon C. Phasic vs sustained fear in rats and humans: role of the extended amygdala in fear vs anxiety. Neuropsychopharmacology. 2010;35:105–135.
71. Sparta DR, Jennings JH, Ung RL, Stuber GD. Optogenetic strategies to investigate neural circuitry engaged by stress. Behav Brain Res. 2013;255:19–25.
72. Sullivan GM, Apergis J, Bush DEA, Johnson LR, Hou M, Ledoux JE. Lesions in the bed nucleus of the stria terminalis disrupt corticosterone and freezing responses elicited by a

contextual but not by a specific cue-conditioned fear stimulus. Neuroscience. 2004;128:7–14.

73. Waddell J, Morris RW, Bouton ME. Effects of bed nucleus of the stria terminalis lesions on conditioned anxiety: aversive conditioning with long-duration conditional stimuli and reinstatement of extinguished fear. Behav Neurosci. 2006;120:324–336.
74. Duvarci S, Bauer EP, Paré D. The bed nucleus of the stria terminalis mediates inter-individual variations in anxiety and fear. J Neurosci. 2009;29:10357–10361.
75. Goode TD, Ressler RL, Acca GM, Miles OW, Maren S. Bed nucleus of the stria terminalis regulates fear to unpredictable threat signals. Elife. 2019;8.
76. Goode TD, Acca GM, Maren S. Threat imminence dictates the role of the bed nucleus of the stria terminalis in contextual fear. Neurobiol Learn Mem. 2020;167:107116.
77. Meloni EG, Jackson A, Gerety LP, Cohen BM, Carlezon WA. Role of the bed nucleus of the stria terminalis (BST) in the expression of conditioned fear. Ann N Y Acad Sci. 2006;1071:538–541.

Figure 1

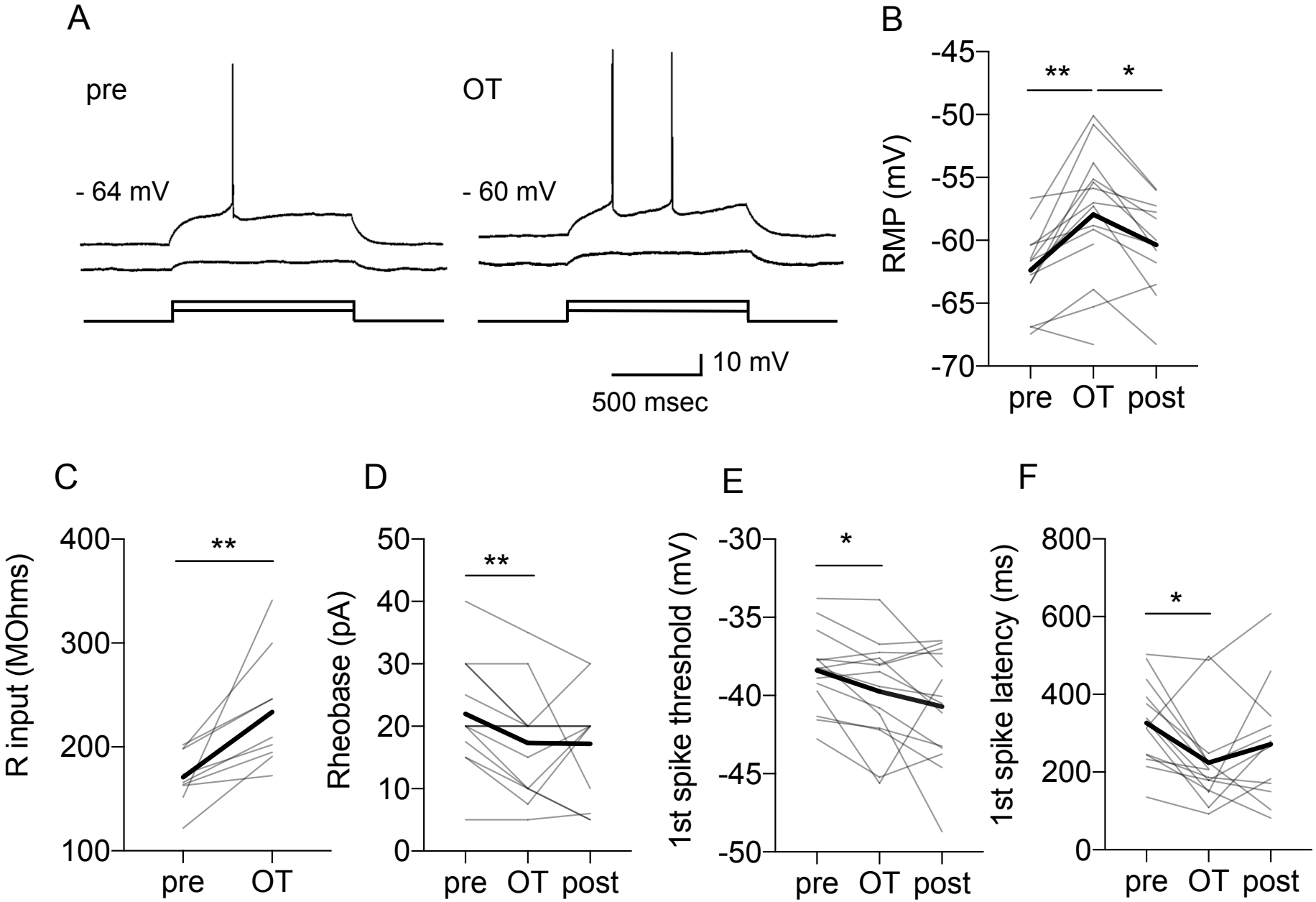
A
pre
- 64 mV
OT
- 60 mV
10 mV
500 msec
B
RMP (mV)
-45
-50
-55
-60
-65
-70
**
*
pre
OT
post
C
R input (MOhms)
400
300
200
100
**
pre
OT
D
Rheobase (pA)
50
40
30
20
10
0
**
pre
OT
post
E
1st spike threshold (mV)
-30
-35
-40
-45
-50
*
pre
OT
post
F
1st spike latency (ms)
800
600
400
200
0
*
pre
OT
post

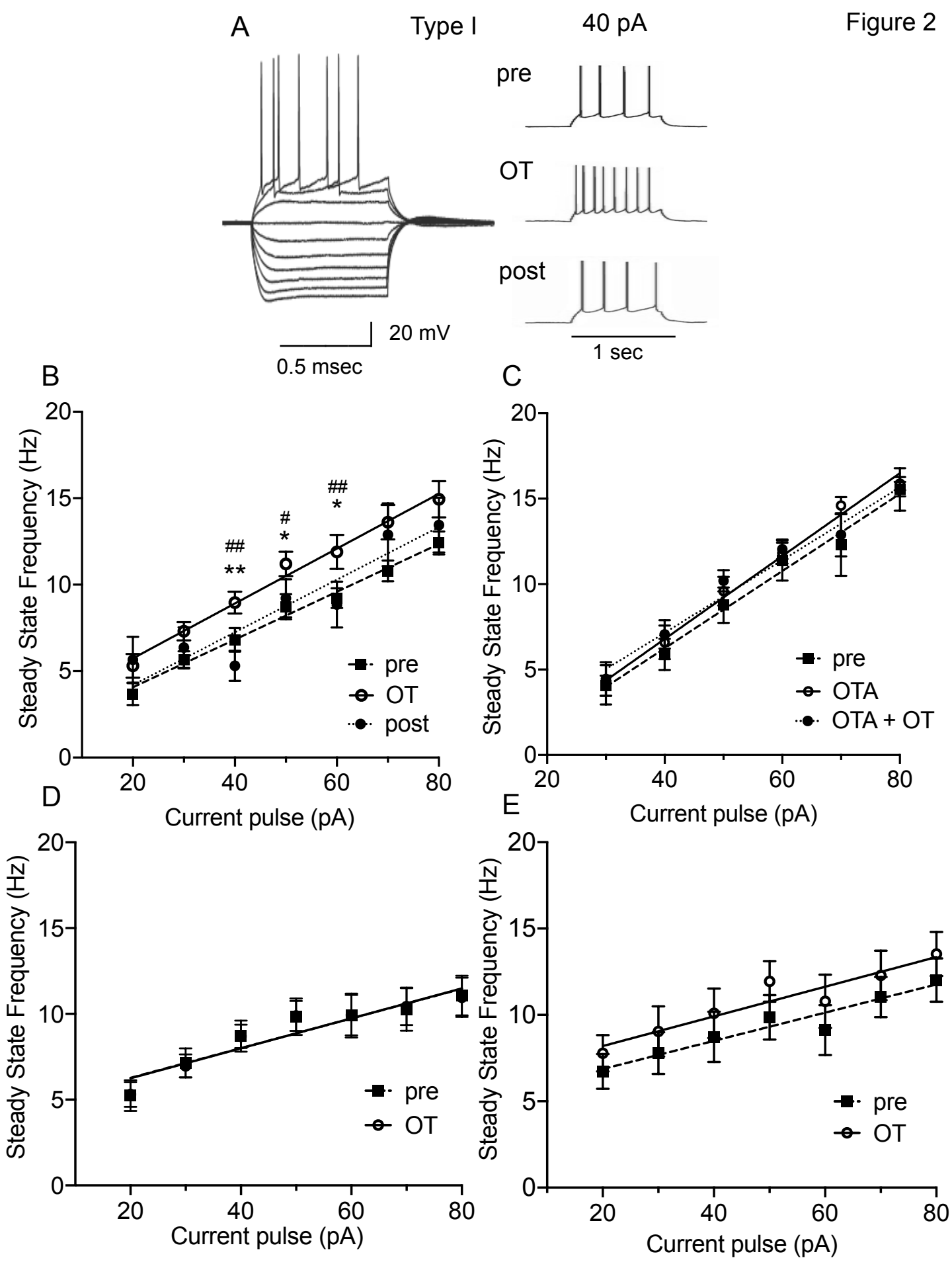
Figure 2
A
Type I
40 pA
pre
OT
post
20 mV
0.5 msec
1 sec
B
Steady State Frequency (Hz)
Current pulse (pA)
pre
OT
post
##
**
#
*
##
*
C
Steady State Frequency (Hz)
Current pulse (pA)
pre
OTA
OTA + OT
D
Steady State Frequency (Hz)
Current pulse (pA)
pre
OT
E
Steady State Frequency (Hz)
Current pulse (pA)
pre
OT

Figure 3

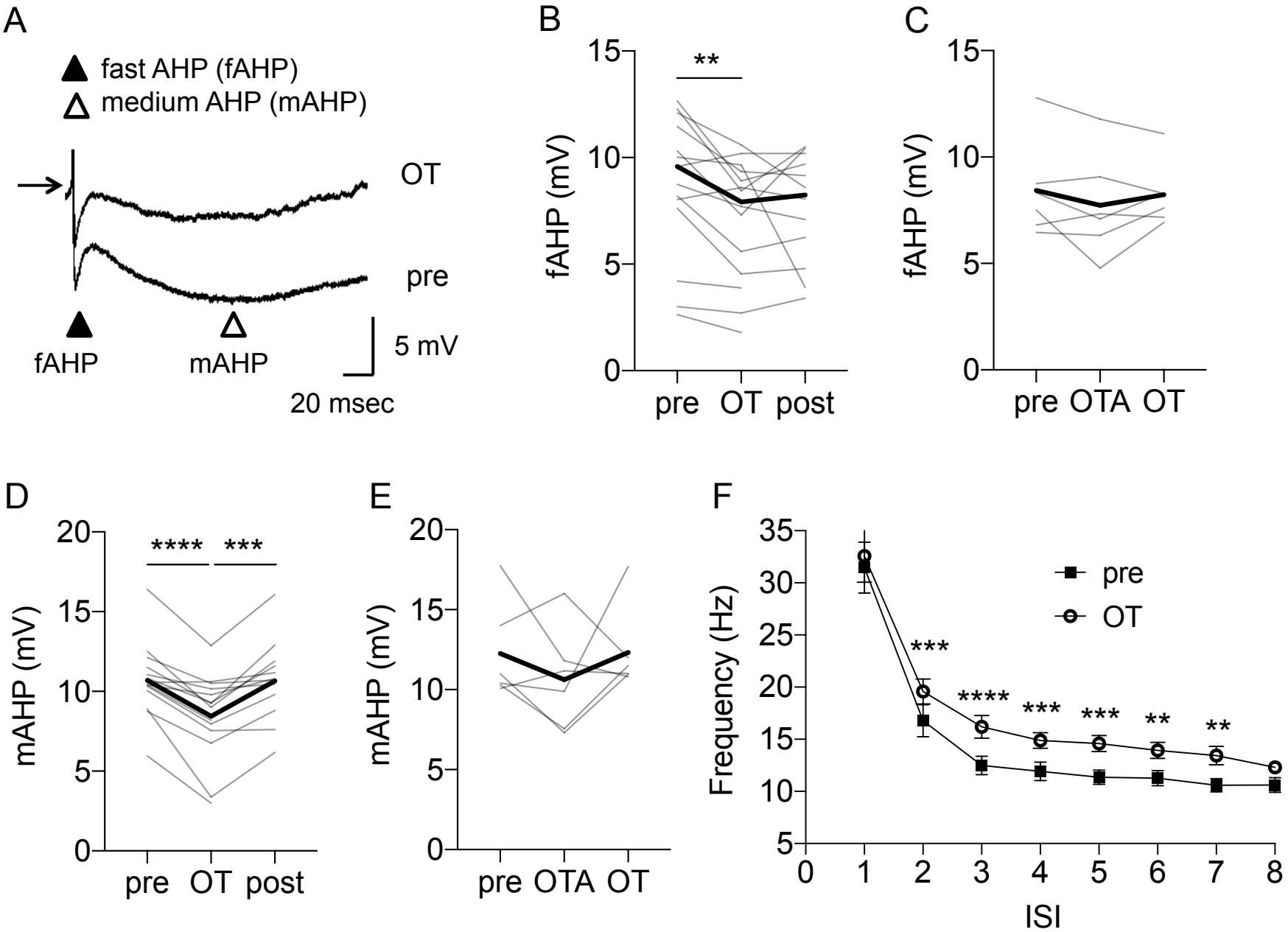
A
fast AHP (fAHP)
medium AHP (mAHP)
OT
pre
fAHP
mAHP
5 mV
20 msec
B
fAHP (mV)
**
pre OT post
C
fAHP (mV)
pre OTA OT
D
mAHP (mV)
**** ***
pre OT post
E
mAHP (mV)
pre OTA OT
F
Frequency (Hz)
pre
OT
***
****
***
***
**
**
ISI

Figure 4

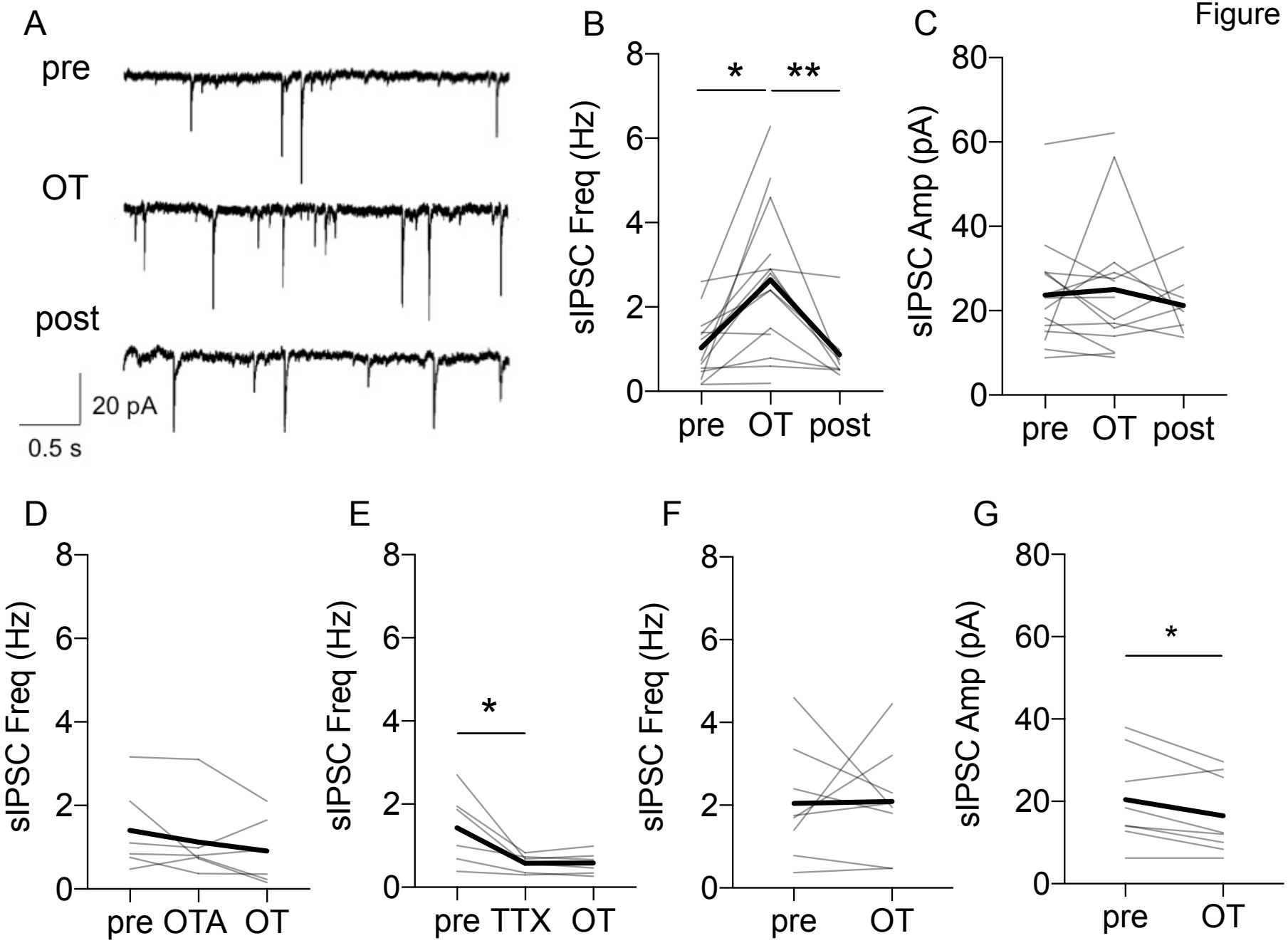
A
pre
OT
post
20 pA
0.5 s
B
sIPSC Freq (Hz)
8
6
4
2
0
*
**
pre
OT
post
C
sIPSC Amp (pA)
80
60
40
20
0
pre
OT
post
D
sIPSC Freq (Hz)
8
6
4
2
0
pre
OTA
OT
E
sIPSC Freq (Hz)
8
6
4
2
0
*
pre
TTX
OT
F
sIPSC Freq (Hz)
8
6
4
2
0
pre
OT
G
sIPSC Amp (pA)
80
60
40
20
0
*
pre
OT

Figure 5

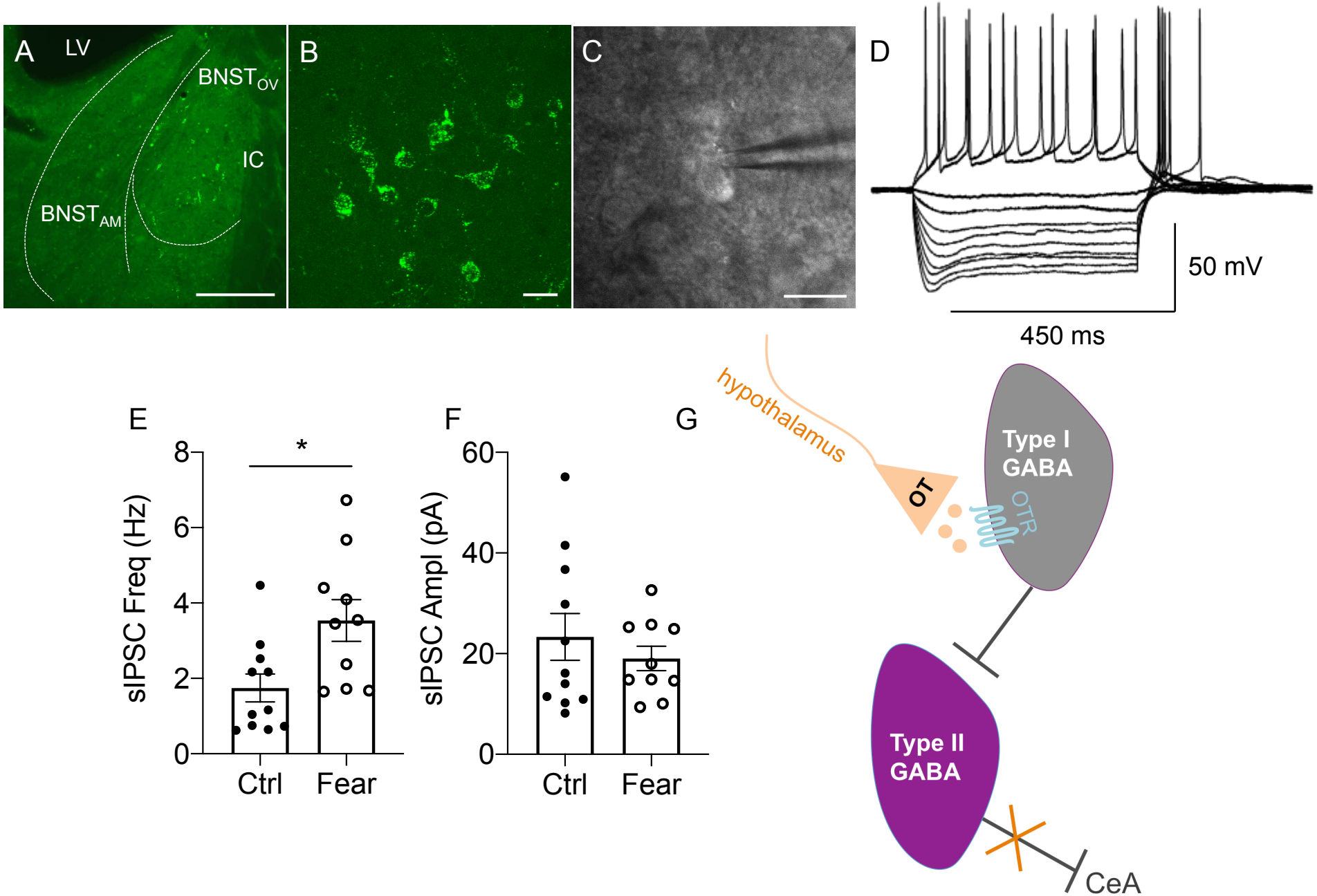
A
LV
BNST$_{OV}$
IC
BNST$_{AM}$
B
C
D
50 mV
450 ms
E
sIPSC Freq (Hz)
8
6
4
2
0
*
Ctrl
Fear
F
sIPSC Ampl (pA)
60
40
20
0
Ctrl
Fear
G
hypothalamus
OT
OTR
Type I GABA
Type II GABA
CeA

Supplementary Information

1. Supplementary materials and methods

1.1. Slice preparation for electrophysiology

Rats were anaesthetized with Isoflurane USP (Patterson Veterinary, Greeley, CO, USA) before decapitation. Brains were quickly removed and coronal 300 µm slices containing the BNST were prepared in ice-cold cutting solution (saturated with 95% O_2/ 5% CO_2) containing in mM: NaCl 130, KCl 3.5, $NaHCO_3$ 30, KH_2PO_4 1.1, $CaCl_2 \cdot 2H_2O$ 1, D-glucose 10, $MgCl_2$ $6H_2O$ 6, Kynurenate 2, pH 7.4, 290-300 mOsm. The slices were prepared using a Leica vibratome (VT1200; Leica, Wetzlar, Germany), then incubated for 1 hr at 34°C in the cutting solution and subsequently transferred to room temperature in artificial cerebrospinal fluid (aCSF) containing in mM: NaCl 130, KCl 3.5, $NaHCO_3$ 30, KH_2PO_4 1.1, $CaCl_2 \cdot 2H_2O$ 2.5, D-glucose 10, and $MgCl_2 \cdot 6H_2O$ 1.3, Ascorbate 0.4, Thiourea 0.8, Na Pyruvate 2, pH 7.4, with osmolarity of 290-300 mOsm, continuously oxygenated with 95% O_2/ 5% CO_2. Next, the slices were transferred to a submerged recording chamber and perfused with aCSF at 33°C ± 1°C saturated with 95% O_2/ 5% CO_2 at a flow rate of 2-3 ml/min. $BNST_{DL}$ neurons were visualized using infrared differential interference contrast (IR-DIC) optic with an Upright microscope (Scientifica SliceScope Pro 1000, Clarksburg, NJ, USA).

1.2. Patch-clamp recordings

Whole-cell patch-clamp recordings were performed from $BNST_{DL}$ neurons using glass pipette (4-8 MΩ) pulled from thick-walled borosilicate glass capillaries with a micropipette puller (Model P-97; Sutter Instrument, Novato, CA, USA). To study the effects of OT on inhibitory synaptic activity the patch pipettes were filled with high chloride internal solution in mM: KOH 110, $MgCl_2 \cdot 6H_2O$ 2, KCl 50, EGTA 0.2, ATP-Na 2,

GTP-Na 0.3, HEPES 10, and Spermine 0.1, the pH was adjusted to 7.3 with D-gluconic acid and osmolarity was 300-305 mOsm. To study the effects of OT on intrinsic membrane properties and firing activity the patch pipettes were filled with potassium gluconate internal solution containing in mM: K-gluconate 135, KCl 2, $MgCl_2 \cdot 6H_2O$ 3, HEPES 10, Na-phosphocreatine 5, ATP-K 2, GTP-Na 0.2, pH 7.3 adjusted with KOH, 300-305 mOsm. Recordings were performed with a Multiclamp 700B amplifier (Molecular Device, Sunnyvale, CA, USA). Current-clamp and voltage-clamp signals were acquired at 10 kHz with a 16-bit input-output board NI USB-6251 (National Instruments, Austin, TX) using custom MatLab scripts (Math-Work, Natick, MA) written by Dr. Niraj Desai (Desai et al., 2017). All neurons included in the analysis had a seal resistance > 1GΩ and an initial access resistance < 20 MΩ maintained for the entire recording period.

1.3. Electrophysiological characterization of $BNST_{DL}$ neurons

At the beginning of the recording sessions in current clamp mode, neurons were electrophysiologically characterized into three types (Type I-III). Based on their characteristic voltage responses (Hammack et al., 2007), three types of neurons were identified in the $BNST_{DL}$. Type I neurons are regular firing and display spike frequency adaptation. These neurons also display moderate voltage sag that indicates the presence of the hyperpolarization-activated cation current (I_h). As a distinguishing feature of Type II neurons, post-inhibitory spikes are produced in response to preceding negative current steps that are related to the action of the low-threshold Ca^{2+} current. Additionally, Type II neurons display strong voltage sags under hyperpolarizing current pulses that indicate a high level of I_h current. Type III neurons differ from the previous two types in several aspects: they exhibit high rheobase and no voltage sag under negative current steps; they display prominent inward rectification that is caused by the

activation of the inward rectifying K^+ current (I_{KIR}) at membrane potentials more negative than approximately −50 mV; and start firing after a characteristic slow voltage ramp.

1.4 Fear-conditioning

Rats were fear-conditioned in acrylic holders inside sound attenuated chambers (San Diego Instruments, Inc., CA). After chamber habituation (day 1, 20 minutes), on the next day fear-conditioned rats were exposed to 10 presentations of a 3.7 s cue light (conditioned stimulus, CS), each co-terminating with a 0.5 s foot shock (unconditioned stimulus, US; 0.5 mA), whereas control rats were placed in the chambers without CS or US exposure.

Supplementary table

Table 1. Intrinsic membrane properties and firing activity of Type I-III $BNST_{DL}$ neurons after OT (0.2 μM) application respective to baseline (pre-OT). ****$P < 0.0001$, **$P < 0.01$, *$P < 0.05$. In Type II neurons OT did not affect RMP ($P = 0.0985$), Rin ($P = 0.1377$), Rh ($P = 0.0964$), or Th ($P = 0.5027$). Similarly, in Type III neurons OT did not significantly change RMP ($P = 0.1066$), Rin ($P = 0.0788$), Rh ($P = 0.1664$), or Th ($P = 0.5150$).

Type I neurons	**Pre**	**OT**
RMP (mV)	-62.39 ± 0.84	**57.94 ± 1.39 ****
Rin (MOhms)	170.98 ± 8.6	**233.64 ± 18.6 ***
Rh (pA)	21.96 ± 2.29	**17.32 ± 2.26 ****
Th (mV)	-38.38 ± 0.68	**39.75 ± 0.88 ***
Lat (ms)	326.44 ± 28.63	**224.58 ± 32.51 ****
fAHP (mV)	8.63 ± 0.89	**7.47 ± 0.77 ****
mAHP (mV)	10.69 ± 0.61	**8.45 ± 0.72 ******
lAHP (mV)	0.49 ± 0.12	0.41 ± 0.1
Type II neurons		
RMP (mV)	-57.04 ± 0.86	-56.74 ± 0.78
Rin (MOhms)	221.8 ± 29.27	276.03 ± 46.66
Rh (pA)	16.92 ± 2.52	15 ± 2.66
Th (mV)	-39.87 ± 0.95	-40.32 ± 1.05
Type III neurons		
RMP (mV)	-65.73 ± 1.42	-63.3 ± 1.83
Rin (MOhms)	120.66 ± 23.12	156.93 ± 29.7
Rh (pA)	56.46 ± 8.92	48.33 ± 7.36
Th (mV)	-37.28 ± 0.85	-37.08 ± 0.93